Real-time analog circuit for auto-correlative weak-value amplification in the time domain: supplemental document

Jing-Hui Huang[a], Guang-Jun Wang[b], and Xiang-Yun Hu[a,*]

[a]Hubei Subsurface Multiscale Image Key Laboratory, School of Geophysics and Geomatics, China University of Geosciences, Lumo Road 388, 430074 Wuhan, China.
[b]School of Automation, China University of Geosciences, Wuhan 430074, China

ABSTRACT

This document provides supplementary information to "Real-time analog circuit for auto-correlative weak-value amplification in the time domain". Here, we display the real printed circuit board and one photo from the AWVA experiment in Section I. In section II, we show the results of the test of the analog multiplier. In section III, we show the results of the test of the analog integrator. In section IV, we show the noise response of AWVA with the real-time analog circuit. In section V, we display the pointer shifts and the auto-correlation intensity of AWVA at different frequencies. In section VI, we display some characteristic results of AWVA at a frequency of 200 Hz with various Gaussian noises.

1. THE REAL PRINTED CIRCUIT BOARD AND ONE PHOTO FROM THE AWVA EXPERIMENT

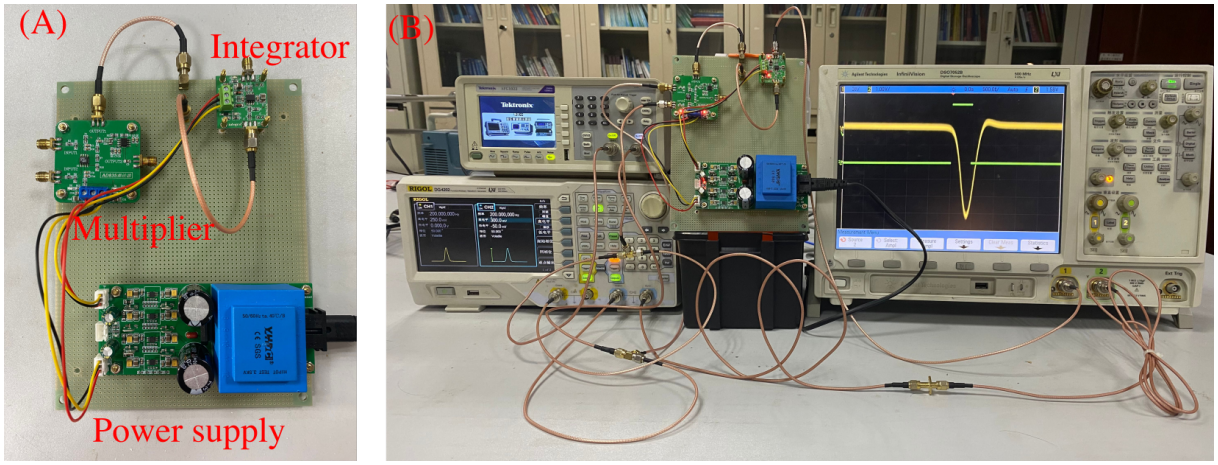

Figure 1. (A) The real printed circuit board (PCB) of the multiplier circuit and the integrator circuit. (B) One Photo from the AWVA experiment.

2. TEST OF THE REAL-TIME ANALOG MULTIPLIER

Testing frequency doubling of the inputs of a sinusoidal signal can be used to evaluate the performance of an analog multiplier.[1] Thus, the multiplication of sinusoidal signals and Gaussian signals is investigated. There is no doubt that the effect of the voltage drop will induce the amplitude of the outputs. And the voltage drop is related to wire material, wire section, distance, load power, ambient temperature, and other factors.[2,3] Therefore, we measured the voltage drop of the different inputs.

Further author information:
Jing-Hui Huang: E-mail: jinghuihuang@cug.edu.cn; Xiang-Yun Hu: E-mail: xyhu@cug.edu.cn

(1) The multiplication of a 0.250 V peak sinusoidal current at 200 Hz and a 0.250 V peak sinusoidal current at 200 Hz is accomplished. In other words, $I_1^{si}(t) = 0.25\sin(2\pi \times 200t)$ V and $I_2^{si}(t) = 0.25\sin(2\pi \times 200t)$ V are selected for multiplication. And the theoretical calculation of the multiplication of sinusoidal signals can be obtained: $\overline{W}^{si}(t) = 0.0625(1 - \cos(2\pi \times 400t))$ V. Therefore, the peak value of theoretical $\overline{W}^{si}(t)$ should be 0.0625 V, and the frequency should be doubled. It can be found that the frequency of the experimental result $W^{si}(t)$ in Fig. 2(B) is doubled. However, the peak value of $W^{si}(t)$ is weaken by the factor $\Gamma_M^{si} \approx 0.0526/0.0625 = 0.842$. In addition, the experimental curve $W^{si}(t)$ has a phase shift compared to the theoretical $\overline{W}^{si}(t)$. This phase shift is induced by capacitance in the analog circuit.

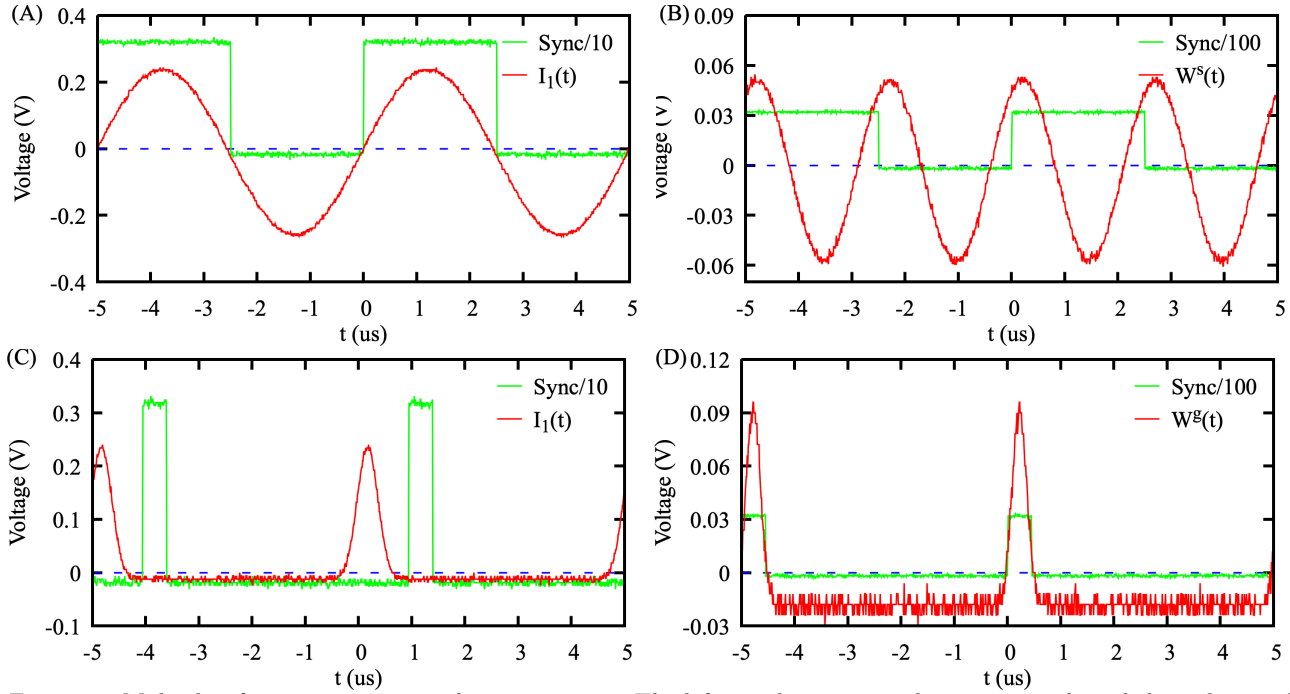

Figure 2. Multiplier frequency response characterization. The left panels represent the input signals and the right panels represent the output signals. The blue dashed line indicates 0 V reference.

(2) To realistically simulate AWVA, the Gaussian pointer/signal is further tested on the Multiplier. The Gaussian input in the Generator is defined by the RIGOL Ultra Station, which can edit the formula of the waveform. The multiplication of a 0.250 V peak Gaussian current at 200 Hz and $I_1^{ga}(t)$ has the form:

$$I_1^{ga}(t) = 0.248\exp\left[-2\left(\frac{t - 1.71 \times 10^{-4}}{3.88 \times 10^{-4}}\right)^2\right] - 0.01 \tag{1}$$

The expression (1) is fit by the Gaussian profile of the input signal. And another input $I_2^{ga}(t)$ takes the same form as the form of $I_1^{ga}(t)$. Note that the Gaussian pules $I_1^{ga}(t)$ in Fig. 2(C) are not continuous in the time domain. The main reason is that the shift of the pointer will affect the value of $W^{ga}(t)$. In other words, every AWVA measurement ought to be independent and can be ensured by a sufficient time between measurements. Finally, the theoretical multiplication of $\overline{W}^{ga}(t)$ can be obtained:

$$\overline{W}^{ga}(t) \approx 0.064\exp\left[-4\left(\frac{t - 1.71 \times 10^{-4}}{3.88 \times 10^{-4}}\right)^2\right] = 0.058\exp\left[-2\left(\frac{t - 2.24 \times 10^{-4}}{2.70 \times 10^{-4}}\right)^2\right]. \tag{2}$$

When signals $I_1^{ga}(t)$ and $I_2^{ga}(t)$ pass through the multiplier, the output is measured as:

$$W^{ga}(t) \approx 0.109\exp\left[-4\left(\frac{t - 2.26 \times 10^{-4}}{2.78 \times 10^{-4}}\right)^2\right]. \tag{3}$$

The experimental result $W^{ga}(t)$ is shown in Fig. 2(D) and the peak value is enhanced by the factor $\Gamma_M^{ga} \approx 0.109/0.058 = 1.87$. Note that the value is larger than $\Gamma_M^{si} = 0.842$ with the input of the sinusoidal signals. Certainly, the factor Γ_M strongly depends on the profile of the input signals.

3. TEST OF THE ANALOG INTEGRATOR

The analog integrator is tested by inputting a square signal $W^{sq}(t)$, a sinusoidal signal $W^{si}(t)$, and a Gaussian signal $W^{ga}(t)$. We set the signal frequency at $\omega = 200$ Hz and period T=5 ms with three types of input signals.

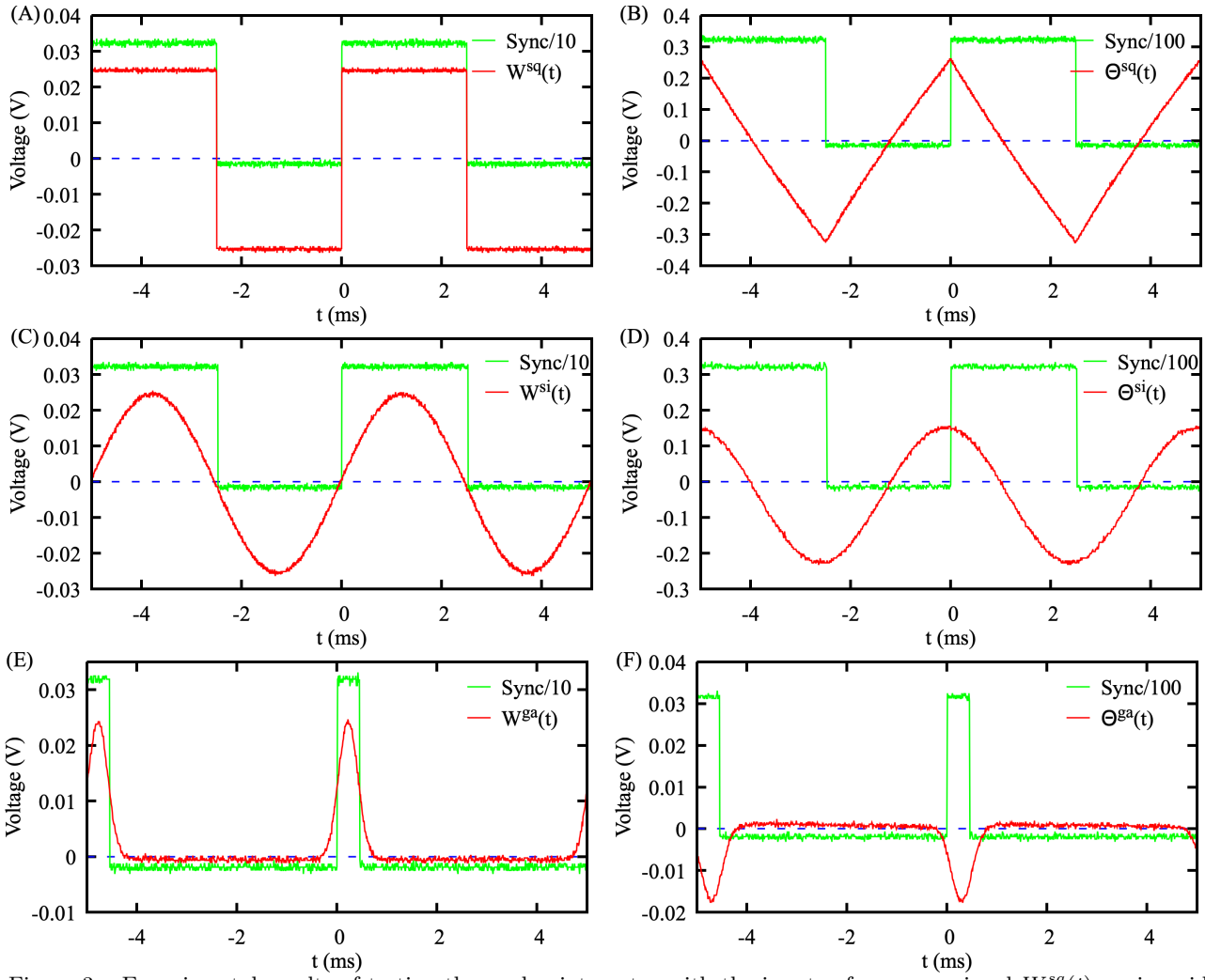

Figure 3. Experimental results of testing the analog integrator with the inputs of a square signal $W^{sq}(t)$, a sinusoidal signal $W^{si}(t)$ and a Gaussian signal $W^{ga}(t)$. The left panels represent the input signal $W(t)$ and the right panels represent the output signal $\Theta(t)$. The blue dashed line indicates 0 V reference.

(1) The integration of a 0.025 V high-level square signal with a 50 % duty cycle is accomplished and shown in Fig. 3. It is known that an analog integrator can change a square wave to a ramp wave. And the theoretical amplitude value $\mathrm{Amp}(\overline{\Theta}^{sq})$ of $\overline{\Theta}(t)$ is proportional to the time period T:

$$\mathrm{Amp}(\overline{\Theta}^{sq}) = \int_0^{T/2} 0.025dt = \int_0^{0.0025} 0.025dt = 6.25 \times 10^{-5} V \tag{4}$$

At the same time, the experimental amplitude value $\mathrm{Amp}(\Theta^{sq}) = 0.6$ V of $\Theta^{sq}(t)$ can be read from Fig. 3(B), and the gain coefficient Γ_I^{sq} of the analog integrator can be calculated by $\Gamma_I^{sq} = 0.6/6.25 \times 10^{-5} = 9600$.

(2) The integration of a 0.025 V high-level sinusoidal signal $W^{si}(t) = 0.025\sin(2\pi \times 200t)V$ is accomplished and shown in Fig. 3(D). Theoretically, the amplitude value $\mathrm{Amp}(\overline{\Theta}^{si})$ of $\overline{\Theta}^{si}(t) = W^{si}(t)$ can be integrated over half period T:

$$\mathrm{Amp}(\overline{\Theta}^{si}) = \int_0^{T/2} \overline{\Theta}^{si}(t)dt = \int_0^{0.0025} 0.025\sin(2\pi \times 200t)dt = 3.97 \times 10^{-5}V \tag{5}$$

From Fig. 3(D) we can directly get the experimental amplitude value $\mathrm{Amp}(\Theta^{si})$= 0.38 V and the gain coefficient Γ_I^{si}= $0.38/3.97 \times 10^{-5}$= 9571.

(3) The integration of a 0.025 V high-level Gaussian signal $W^{ga}(t)$ is measured, and the experimental result of $W^{ga}(t)$ shown in Fig. 3(E) has the form:

$$W^{ga}(t) = 0.248\exp\left[-2\left(\frac{t - 2.19 \times 10^{-4}}{3.67 \times 10^{-4}}\right)^2\right] - 0.0004 \tag{6}$$

Note that the integration of the analog integrator is quite different from the mathematical integral since the increment of the integral is associated with the variation of voltage over time. A change in the slope of the curves $W(t)$ results in a change in the sign of the integral. Therefore, the theoretical maximum value $\mathrm{Max}(\overline{\Theta}^{ga})$ can be obtain at the central value t_0= $2.19 \times 10^{-4}s$:

$$\begin{aligned}
\mathrm{Max}(\overline{\Theta}^{ga}) &= \int_0^{t_0} W^{ga}(t)dt \\
&= \int_0^{2.19\times10^{-4}} \left(0.248\exp\left[-2\left(\frac{t - 2.19 \times 10^{-4}}{3.67 \times 10^{-4}}\right)^2\right] - 0.0004\right)dt \\
&= 4.25 \times 10^{-6}V
\end{aligned} \tag{7}$$

Meanwhile, the experimental maximum value $\mathrm{Max}(\Theta^{ga})$= 0.019 V can be read from Fig. 3(F). Then the gain coefficient can be calculated by Γ_I^{ga}= $0.019/4.25 \times 10^{-6}$= 4470.

In general, we can obtain the overall gain coefficient $\Gamma = \Gamma_M \times \Gamma_I$ (*e.g.* $\Gamma^{ga} = \Gamma_M^{ga} \times \Gamma_I^{ga}$= 1.87× 4470= 8358) from the theoretical calculation and experimental estimation of the auto-correlation intensity Θ(t). It can be found that the value of Γ is much larger than one, and the gain coefficient depends on the profile of the input signal. In addition, the enhancement of signal amplitude is encouraging since the post-selection in AWVA inevitably reduces the probability of a successful post-selection.[4,5]

4. THE NOISE RESPONSE OF AWVA WITH THE REAL-TIME ANALOG CIRCUIT

We further test the noise responses of AWVA with the real-time analog circuit, and the results with different time windows are shown in Fig. 4. In principle of the auto-correlation technique for signal denoising in engineering,[6–8] the auto-correlation intensity $\Theta_{\mathrm{NN}}(\mathrm{t};\tau)$ of the Gaussian white noise $\mathbf{N}(t, N_A)$ is defined as:

$$\Theta_{\mathrm{NN}}(t) = \int_0^t \mathbf{N}(t', N_A) \times \mathbf{N}(t', N_A)dt' = 0\,(t \to \infty)\,. \tag{8}$$

where N_A is the amplitude of the Gaussian noise. In our test, the Gaussian noise is generated by another Function Generator (Tektronix AFG1022, 25 MHz, 125 MS/s). For demonstrating the robustness of AWVA, the amplitude of the Gaussian noise is also set at N_A= 500 mV with zero mean value. Where the amplitude of the noise is the same as the pointer $I(t)$.

The result of the auto-correlation intensity $\Theta_{\mathrm{NN}}(\mathrm{t})$ with the input Gaussian white noise $\mathbf{N}(t, N_A)$ is displayed in Figs. 4(E) and 4(F). While Figs. 4(C) and 4(D) display the FFT results of signals $I_1^N(t)$ and $I_2^N(t)$. The left panels and the right panels show the different windows of the measurement time of the Scope. When inputting the noises with amplitude N_A = 500 mA, the amplitude of the noise response $\Theta_{NN}(t)$ is about 6 mV. It can be

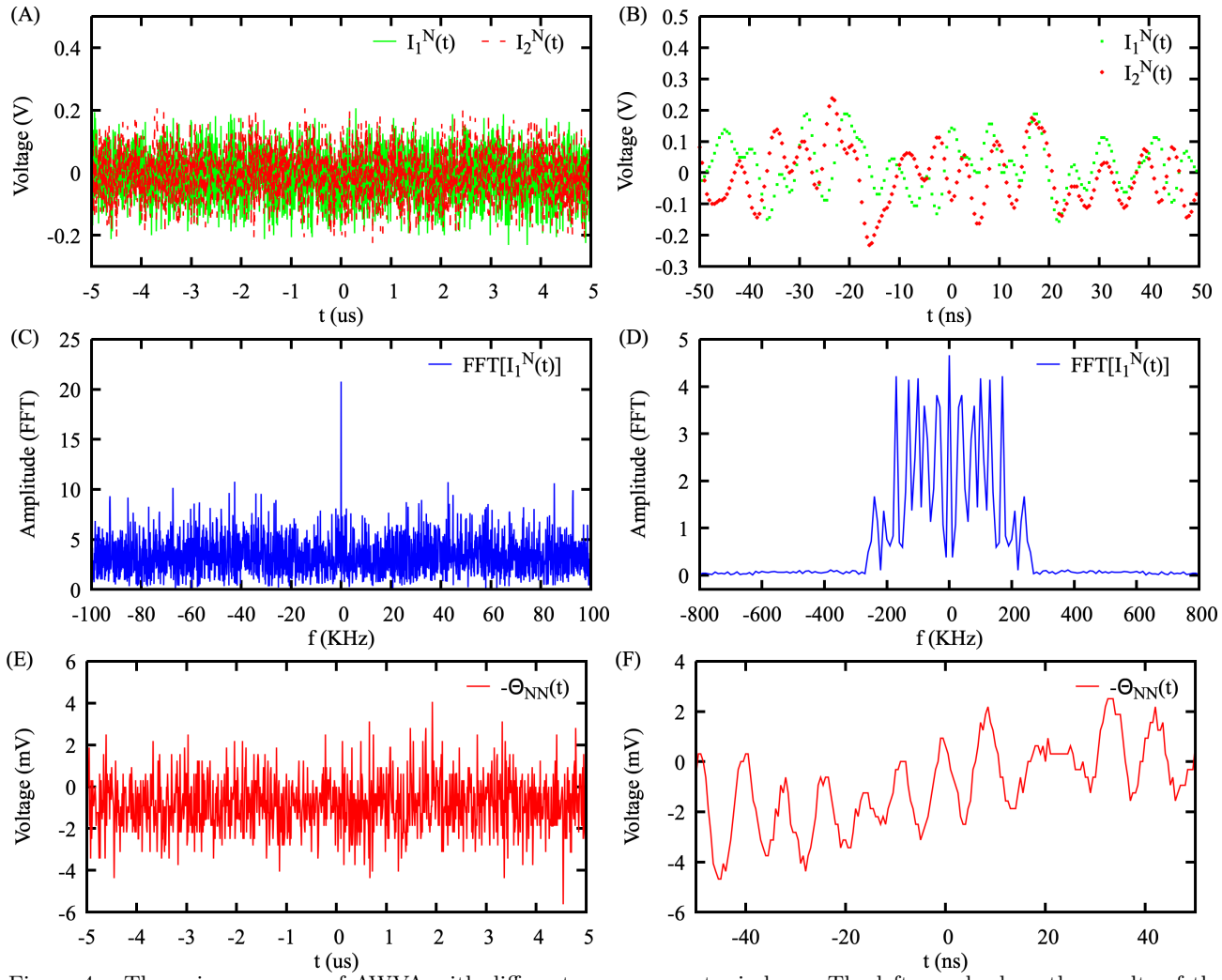

Figure 4. The noise response of AWVA with different measurement windows. The left panels show the results of the measurement with the window -5 us $<$ t $<$ 5 us. The right panels show the results of the measurement with the window -50 ns $<$ t $<$ 50 ns. Note that the data is taken from a single measurement of the Scope.

found that the amplitude of $\Theta_{NN}(t)$ is much smaller than the values of Max[$\Theta_{\rm IN}$(t)] with the AWVA signal at frequencies f=200 Hz and f=2000 Hz.

In addition, the result in Fig. 4(F) indicates that the value of $\Theta_{NN}(t;\tau)$ oscillates over the measurement window -50 ns $<$ t $<$ 50 ns and it is hard to estimate the mean value of the $\Theta_{\rm NN}$(t). The main reason is that the small measurement window does not contain enough sample points. Therefore, as shown in Fig. 4(E), a stable mean value of $\Theta_{NN}(t)$ can be obtained by increasing the measurement window or the measurement time. Note that the mean value of the $\Theta_{\rm NN}$(t) is about -1 mV and is not exactly equal to zero according to Eq. (8). Certainly, this deviation of the mean value can be regarded as a system error in our circuit. In summary, the results of Gaussian noises indicate that Gaussian noises have a slight influence on AWVA when the frequency of the pointer is set at f=200 Hz and 2000 Hz.

5. THE POINTER SHIFTS AND THE AUTO-CORRELATION INTENSITY OF AWVA AT DIFFERENT FREQUENCIES

Fig. 5 displays a single measurement of $\Theta(t;\delta t)$ when detecting different time shifts of signals $I_1^G(t)$ and $I_2^G(t)$ at various frequencies.

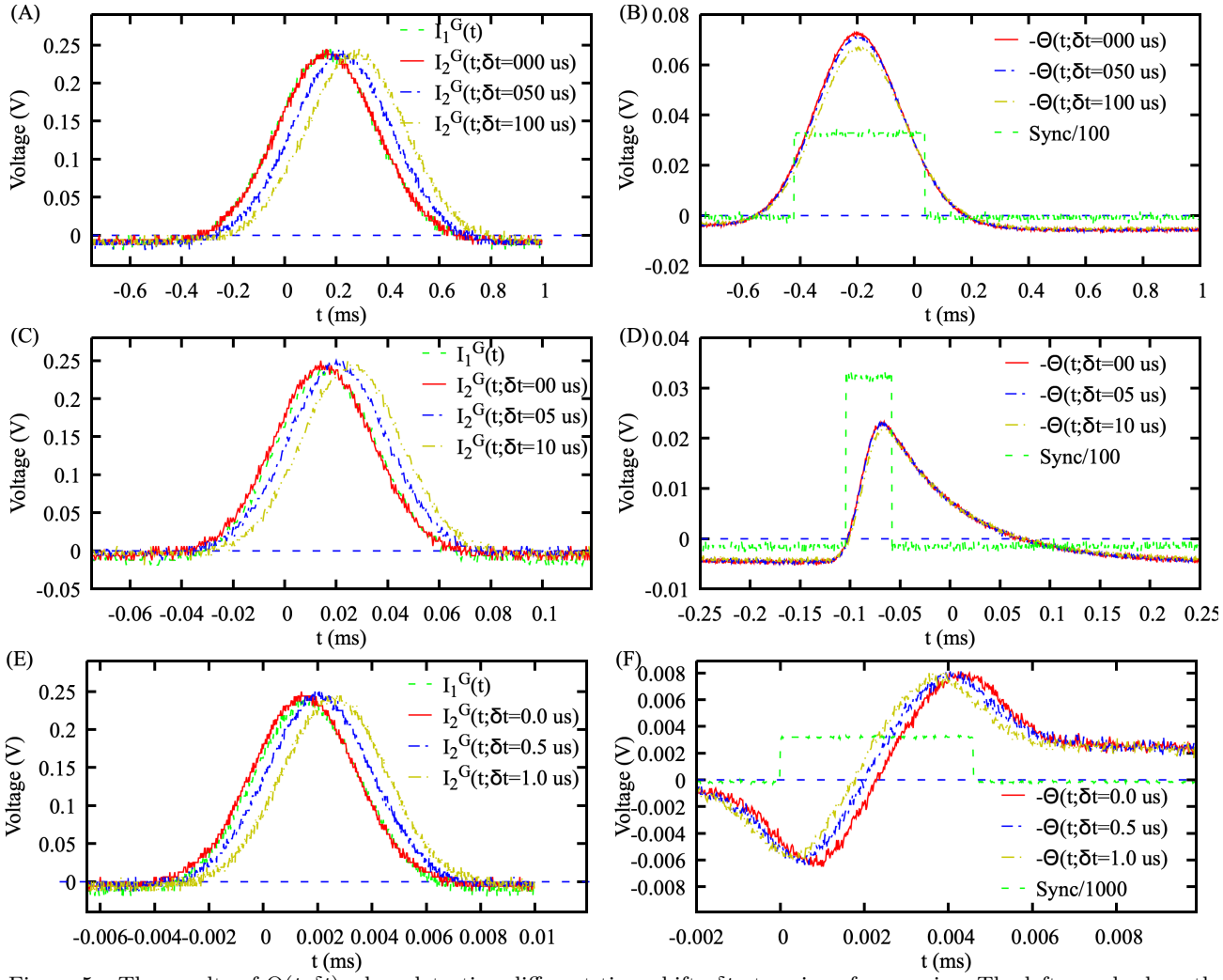

Figure 5. The results of $\Theta(t;\delta t)$ when detecting different time shifts δt at various frequencies. The left panels show the input of signals $I_1^G(t)$ and $I_2^G(t)$ and the right panels show the experimental curve $\Theta(t;\delta t)$ with different time shifts of the pointer. (A) and (B) represent the measurement at frequency f= 200 Hz. (C) and (D) represent the measurement at frequency f= 2000 Hz. (E) and (F) represent the measurement at frequency f= 20000 Hz. The blue dashed line indicates 0 V reference.

6. CHARACTERISTIC RESULTS OF AWVA AT A FREQUENCY OF 200 HZ WITH VARIOUS GAUSSIAN NOISES

When implementing AWVA with the real-time analog circuit under strong Gaussian noise, the measurements with different amplitudes of noise are investigated. We show the mean value of Max$[\Theta(t;\delta t)]$ and Max$[\Theta(t)]$ as well as the corresponding sensitivity in Table 1. In this paper, the data of N_A= 2 mV is assumed to be the results of the measurement without noise.

Table 1. Parameters and some characteristic results for measuring the time shifts δt= 50 us at frequency f= 200 Hz when adding Gaussian noise with different amplitude N_A (mV). The time delay δt^{Scope} (us), the maximum value Max$[\Theta(t;\delta t)]$ (mV), and the maximum value Max$[\Theta(t)]$ (mV) are directly read out as the time delay and the maximum values with their stand standard deviation from the scope. The count number C, which corresponds to the number of the measurement, is sufficient ($C > 10000$ times) for obtaining a stable mean value.

N_A	δt^{Scope}	Max$[\Theta_{IN}(t)]$	Max$[\Theta_{IN}(t;\delta t)]$	K (10^{-2} mV/us)
2 ($\approx$ 0)	50 ± 4.7	20.622 ± 0.113	20.018 ± 0.181	1.208 ± 0.588
10	51 ± 2.3	20.661 ± 0.157	20.082 ± 0.153	1.158 ± 0.620
20	51 ± 3.7	20.728 ± 0.185	20.155 ± 0.175	1.146 ± 0.720
30	52 ± 4.4	20.856 ± 0.199	20.245 ± 0.231	1.222 ± 0.860
40	50 ± 4.5	21.015 ± 0.141	20.452 ± 0.238	1.126 ± 0.758
50	52 ± 6.7	21.082 ± 0.160	20.512 ± 0.194	1.140 ± 0.708
60	49 ± 7.3	21.131 ± 0.189	20.586 ± 0.134	1.090 ± 0.646
70	53 ± 11	21.243 ± 0.172	20.755 ± 0.203	0.976 ± 0.750
80	60 ± 14	21.434 ± 0.159	20.827 ± 0.210	1.214 ± 0.738
90	62 ± 15	21.530 ± 0.228	21.015 ± 0.170	1.030 ± 0.796
100	45 ± 22	21.865 ± 0.209	21.231 ± 0.216	1.268 ± 0.850
200	52 ± 23	23.463 ± 0.290	22.833 ± 0.279	1.261 ± 1.138
300	44 ± 47	25.370 ± 0.404	24.775 ± 0.354	1.191 ± 1.516
400	33 ± 145	27.102 ± 0.453	26.465 ± 0.420	1.274 ± 1.746
500	101 ± 545	29.077 ± 0.535	28.405 ± 0.524	1.344 ± 2.180
600	112 ± 603	30.913 ± 0.556	30.110 ± 0.589	1.606 ± 2.295
700	205 ± 652	32.641 ± 0.716	31.904 ± 0.638	1.474 ± 2.708
800	30 ± 470	34.482 ± 0.744	33.691 ± 0.801	1.582 ± 3.090
900	16 ± 400	36.177 ± 0.897	35.322 ± 0.861	1.110 ± 3.516
1000	23 ± 314	37.995 ± 1.123	36.956 ± 1.002	2.078 ± 4.256
1200	6 ± 288	41.332 ± 1.814	40.447 ± 1.633	1.770 ± 6.894
1400	-25 ± 345	44.823 ± 2.485	43.923 ± 2.458	1.800 ± 9.886
1600	18 ± 273	48.348 ± 3.768	47.612 ± 3.470	1.472 ± 14.47
1800	-93 ± 384	51.664 ± 5.634	50.932 ± 5.424	1.464 ± 22.11
2000	-61 ± 369	54.764 ± 8.157	54.085 ± 7.936	1.358 ± 32.18

REFERENCES

[1] Yuce, E., "Design of a simple current-mode multiplier topology using a single cccii+," *IEEE Transactions on Instrumentation and Measurement* **57**(3), 631–637 (2008).

[2] Guarcello, C., Filatrella, G., Spagnolo, B., Pierro, V., and Valenti, D., "Voltage drop across josephson junctions for lévy noise detection," *Phys. Rev. Research* **2**, 043332 (Dec 2020).

[3] Shekhar, A., Ramírez-Elizondo, L., Bandyopadhyay, S., Mackay, L., and Bauera, P., "Detection of series arcs using load side voltage drop for protection of low voltage dc systems," *IEEE Transactions on Smart Grid* **9**(6), 6288–6297 (2018).

[4] Ferrie, C. and Combes, J., "Weak value amplification is suboptimal for estimation and detection," *Phys. Rev. Lett.* **112**, 040406 (Jan 2014).

[5] Knee, G. C. and Gauger, E. M., "When amplification with weak values fails to suppress technical noise," *Phys. Rev. X* **4**, 011032 (Mar 2014).

[6] Lee, Y., Cheatham, T., and Wiesner, J., "Application of correlation analysis to the detection of periodic signals in noise," *Proceedings of the IRE* **38**(10), 1165–1171 (1950).

[7] Liu, Y., Liu, J., and Kennel, R., "Frequency measurement method of signals with low signal-to-noise-ratio using cross-correlation," *Machines* **9**(6) (2021).

[8] Takahashi, E. J., Lan, P., Mücke, O. D., Nabekawa, Y., and Midorikawa, K., "Attosecond nonlinear optics using gigawatt-scale isolated attosecond pulses," *Nature Communications* **4**(1), 2691 (2013).